The Representation of Cumulus Convection in High-Resolution Simulations of the 2013 Colorado Front Range Flood

KELLY M. MAHONEY

Physical Sciences Division, NOAA/Earth Systems Research Laboratory, Boulder, Colorado

(Manuscript received 7 June 2016, in final form 11 August 2016)

ABSTRACT

Model simulations of the 2013 Colorado Front Range floods are performed using 4-km horizontal grid spacing to evaluate the impact of using explicit convection (EC) versus parameterized convection (CP) in the model convective physics "gray zone." Significant differences in heavy precipitation forecasts are found across multiple regions in which heavy rain and high-impact flooding occurred. The relative contribution of CP-generated precipitation to total precipitation suggests that greater CP scheme activity in areas upstream of the Front Range flooding may have led to significant downstream model error.

Heavy convective precipitation simulated by the Kain–Fritsch CP scheme in particular led to an alteration of the low-level moisture flux and moisture transport fields that ultimately prevented the generation of heavy precipitation in downstream areas as observed. An updated, scale-aware version of the Kain–Fritsch scheme is also tested, and decreased model errors both up- and downstream suggest that scale-aware updates yield improvements in the simulation of this event. Comparisons among multiple CP schemes demonstrate that there are model convective physics gray zone considerations that significantly impact the simulation of extreme rainfall in this event.

1. Introduction

a. *Numerical model assessments of the 2013 Colorado Front Range flood*

During the week of 9–16 September 2013, record-breaking rainfall and historic flooding occurred over portions of the Rocky Mountain Front Range region of northern Colorado. Unusually widespread and long-lasting rainfall led to at least 8 fatalities, greater than $2 billion (U.S. dollars) worth of damage, washed-out highways, isolated communities, and triggered 18 federal disaster declarations across the Colorado Front Range. Various meteorological, impacts-based, and forecast analyses of this event appear in recent literature: Lavers and Villarini (2013), Hamill (2014), Schwartz (2014), Gochis et al. (2015), Mahoney et al. (2015), Morales et al. (2015), Friedrich et al. (2016), and others.

Forecast skill of this event has been assessed by Lavers and Villarini (2013), Hamill (2014), and Schwartz (2014). Lavers and Villarini (2013) focus on coarser-scale global forecast systems, Hamill (2014) focuses on both global systems as well as some mesoscale systems, and Schwartz (2014) demonstrates that forecast skill improves in high-resolution (1-km grid spacing) simulations. These studies conclude that while select operational model forecast systems generated significant precipitation for this event, errors in precipitation intensity, timing, and placement, in addition to model performance trends worsening in time, degraded the event's overall predictability. Findings from these studies also indicate that higher model resolution—and in particular, model ensembles run at higher resolution—may have offered enhanced guidance to human forecasters.

In light of the 2013 Front Range floods, along with other recent high-impact weather events, there is mounting community support for the development of operational convection-allowing ensemble modeling systems, and thus such systems are likely to become more common in the operational forecast environment in the next few years (e.g., Clark et al. 2009, 2012; Schwartz et al. 2015). It is most likely that such ensembles will be run at 3–4-km grid spacing (e.g., Schwartz et al. 2015; Golding et al. 2016).

The 4-km grid spacing is often considered a relatively "high-resolution," acceptable grid spacing threshold at

Corresponding author address: Kelly M. Mahoney, Physical Sciences Division, NOAA/Earth Systems Research Laboratory, 325 Broadway, Boulder, CO 80305.
E-mail: kelly.mahoney@noaa.gov

DOI: 10.1175/MWR-D-16-0211.1

which convective parameterization (CP) can be turned off for forecasts of organized convection; this assumes that the model is capable of explicitly resolving convection on the grid scale (e.g., Weisman et al. 1997; Kain et al. 2008 among many others). However, in recent years many studies and efforts to improve model forecasts run at increasingly higher resolutions have questioned this assumption (e.g., Bryan et al. 2003; Deng and Stauffer 2006; Lean et al. 2008; Bengtsson et al. 2012; Gerard 2015). In fact, for certain applications, there remains considerable effort under way to adapt and improve convective parameterization scheme (CPS) performance at these scales (e.g., Gerard 2015; Bengtsson and Körnich 2016; Zheng et al. 2016).

b. Convective parameterization at "storm-resolving" scales

The model deep convection "gray zone" can be described as the range of scales where model parameterization of deep convection requires adaptation because some of the macro- and microscale parameterization assumptions break down, yet grid spacing is still too coarse to fully resolve deep convection. Key CP assumptions that break down with increasing horizontal resolution include limitations of a "gridbox" state (i.e., a growing importance of horizontal fluxes and the need for communication with neighboring grid points), cloud life cycle/temporal mismatches and overlapping with explicitly resolved convection leading to double counting of precipitation, and questionable suitability of large-scale microphysics formulations. Bounds on the gray zone tend to vary with specific phenomenon, region, season, model, and application, but generally encompass a range from ~1- to 5-km horizontal grid spacing. Many studies have shown that some degree of CP may be necessary at grid lengths down to ~1 km or even finer (e.g., Kuo et al. 1997; Petch et al. 2002; Bryan et al. 2003; Lean et al. 2008; Bengtsson and Körnich 2016).

Though trade-offs of CP in the gray zone have been documented, many studies have shown clear benefits of employing CP at relatively fine grid spacings. For instance, employing CP may help to avoid unrealistic buildup of CAPE, as well as spurious convection realized through gridpoint storms (Zhang et al. 1988; Mahoney et al. 2013). Deng and Stauffer (2006) demonstrated that the skill of a 4-km simulation suffered when no CP was used, because the convective updrafts accompanying a cold frontal system were forced on coarser-than-observed scales, and the rainfall and the atmospheric response to the convection became too strong. The use of cloud microphysics parameterization alone (without active CP) at high resolutions may also not be sufficient to represent moist convection and precipitation in certain regimes (e.g., Molinari and Dudek 1992; Seaman et al. 1998; Cintineo et al. 2014; Zheng et al. 2016). Furthermore, many CPSs include a shallow mixing component, the omission of which can lead to issues such as spurious stratus cloud cover unless those shallow mixing processes are accounted for elsewhere in the model [e.g., in a planetary boundary layer parameterization scheme; Lackmann (2011)].

However, despite the numerous caveats that emerge when transitioning to explicit convection, many studies clearly demonstrate that squall lines, propagating systems, and heavy precipitation events are generally handled poorly by CP and are better served by explicit convection even at relatively coarse resolution (e.g., Weisman et al. 1997; Done et al. 2004; Bukovsky et al. 2006; Kain et al. 2008; Weisman et al. 2008). Additionally, Mahoney and Lackmann (2007) demonstrated that CP activity can have detrimental effects not only on a convective system forecast itself, but also on downstream precipitation forecast skill due to unrealistic representation of the organized upstream convection.

As demonstrated by many of the aforementioned previous studies on the model deep convection gray zone, the problem in merely applying CP in the gray zone as a "catch-all" for those processes that would not be well handled on the grid scale is that many CP schemes have not been adequately adapted for finer grid scales. Open questions remain as to what extent subgrid-scale CP could or should be modified to incorporate "scale awareness" toward improving high-resolution model simulation of extreme precipitation. And even in situations where a scale-aware scheme is clearly desired, the practical issue of a current lack of readily available options of such schemes can also force users into making selections that may be ill-suited for a specific model resolution or user need. In this study, we take CP schemes that have been formulated for and used across various scales and employ them at 4-km grid spacing. We specifically include a newly developed scheme [the multiscale Kain–Fritsch scheme; Zheng et al. (2016)], which includes modifications designed to account precisely for many of the scale-aware needs listed above.

The 2013 Colorado Front Range floods are of particular phenomenological interest from the model gray zone perspective, due to the extended spatial and temporal scale of the heavy precipitation that occurred during this event. This breadth in space and time suggests strong, systematic environmental forcing that might be well suited for some CP scheme strengths, while key intense convective episodes during the event demonstrated more mesoscale-organized convective structures that are generally considered to be best

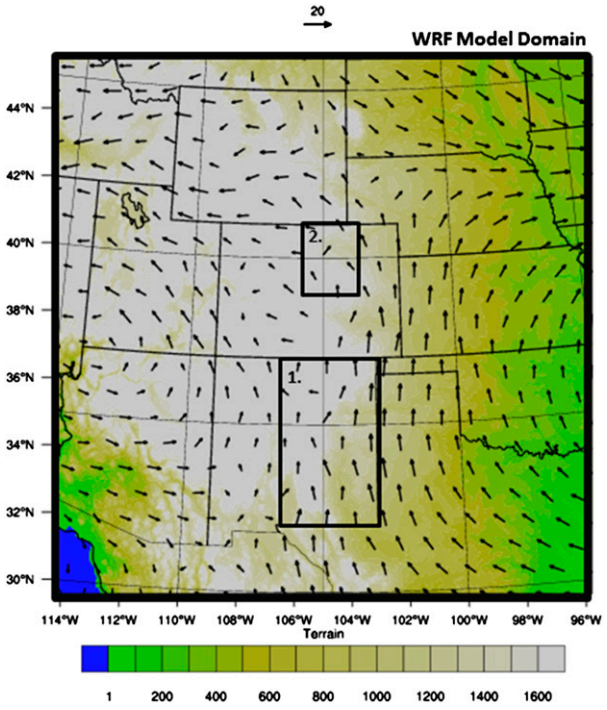

FIG. 1. Map of the west-central United States showing the WRF Model domain (full display region), and inset boxes 1 and 2 showing regions for averaging over (upstream) ENM and (downstream) COFR, respectively. Vectors show EC-simulation 700-hPa wind speed ($m\,s^{-1}$; reference vector in upper center of plot) and direction valid at 1800 UTC 11 Sep.

captured explicitly. In a general sense, one would suspect that a CP scheme may have some benefit at 4-km grid spacing if small convective elements could not be sufficiently resolved; however, the larger-scale environmental adjustments resulting from unnecessary or overactive CP scheme activity may also adversely affect in situ and/or downstream precipitation generation (e.g., Mahoney and Lackmann 2007). Furthermore, that a significant fraction of the flood-producing precipitation in the Colorado Front Range was terrain focused (Morales et al. 2015) might suggest less opportunity for CP or explicit precipitation error (relative to convection that forms and moves independently of static terrain features); yet as mentioned above, significant errors were observed at many forecast space and time scales.

In this study several community-available CP schemes are tested at 4-km grid spacing for simulations of the 2013 Colorado Front Range Flood in order to investigate the representation of convection both upstream and in the location of observed flooding. The objective of this study is to evaluate the relative benefits of convective parameterization and explicit convection for the 2013 Front Range Flood in the 4-km grid spacing model deep convection gray zone.

2. Methods

The Weather Research and Forecasting (WRF) Model, version 3.7.1 (Skamarock et al. 2008) was run using 4-km horizontal grid spacing over a region encompassing most of the intermountain western United States (Fig. 1, Table 1). Subregions over New Mexico and Colorado are also defined in Fig. 1; these regions are used for spatial averaging and subregional analysis in later sections. As illustrated by low-level wind vectors, one can also define these subregions as ''upstream'' (over eastern New Mexico) and ''downstream'' (the Colorado Front Range).

The simulations were initialized at 0000 UTC 11 September 2013 (approximately 24 h before the period of heaviest precipitation began) and run for 72 h in duration. Initial and lateral boundary conditions used the NCEP Climate Forecast System Reanalysis (CFSR; Saha et al. 2010). Model details and physics selections are detailed in Table 1, and Table 2 outlines the CP experiments in which the following CP schemes were employed: Kain–Fritsch (KF), multiscale Kain–Fritsch (MSKF), Grell–Freitas (GF), Betts–Miller–Janjić (BMJ), old GFS simplified Arakawa–Schubert (SAS-old), and new GFS simplified Arakawa–Schubert (SAS-new), in addition to the explicit convection (EC) simulation run without any CPS.

Of particular note for this study is the testing of the new, updated MSKF scheme following Zheng et al. (2016). The

TABLE 1. WRF Model specifications for all simulations.

Model version	WRF (ARW), version 3.7.1
Duration	72 h; 0000 UTC 11 Sep 2013–0000 UTC 14 Sep 2013; output frequency: 1 h
Grid	4-km horizontal grid spacing; 54 vertical levels
	450 × 450 gridpoint domain
Initial and boundary conditions	NCEP CFSR; boundary conditions updated every 6 h
Model physics	Thompson microphysics
	YSU planetary boundary layer (PBL) scheme
	Unified Noah land surface model, revised MM5 Monin–Obukhov surface layer physics
	Dudhia, RRTM radiation physics

TABLE 2. WRF Model experiments according to convective parameterization selections.

Treatment of convective parameterization	Expt name
Explicit convection (no convective parameterization used)	EC
Kain–Fritsch (new Eta) scheme (Kain and Fritsch 1993)	KF
Multiscale Kain–Fritsch scheme (Zheng et al. 2016)	MSKF
Betts–Miller–Janjić scheme (Janjić 1994)	BMJ
Grell–Freitas ensemble scheme (Grell and Freitas 2013)	GF
Old GFS simplified Arakawa–Schubert scheme (Pan and Wu 1995)	SAS-old
New GFS simplified Arakawa–Schubert scheme (Han and Pan 2011)	SAS-new

MSKF incorporates scale-aware parameterized cloud dynamics for high-resolution forecasts by making several changes to the KF CPS in the WRF Model. These changes include subgrid-scale cloud–radiation interactions, a scale-dependent dynamic adjustment time scale, impacts of cloud updraft mass fluxes on grid-scale vertical velocity, and lifting condensation level–based entrainment methodology that also includes scale dependency. Other scale-dependent parameters include fallout rate of condensates from updrafts and stabilization of cloud layers through removal of CAPE. In addition, the MSKF scheme avoids double counting of precipitation. Additional details regarding the development of the MSKF can be found in Herwehe et al. (2014), Alapaty et al. (2015), and Zheng et al. (2016); while those studies demonstrate improvements in forecast skill for certain applications, the focus was not on extreme precipitation as is examined here.

3. Results

a. *Precipitation differences between EC and all CP experiments*

Three-day precipitation totals from the simulation run with EC compare quite well overall with both gridded precipitation observations available from the stage-IV product (Lin and Mitchell 2005; Figs. 2, 3, and 4), as well as regionwide gauge observations (Gochis et al. 2015; Mahoney et al. 2016). While radar-based observations have limitations for this case [as well as for most extreme precipitation events that occur in complex terrain; Gochis et al. (2015)], precipitation maxima are generally simulated quite accurately with respect to available observations of intensity and location (particularly in both eastern New Mexico and the Colorado Front Range region; Figs. 2–4). Thus, the EC simulation may be effectively considered a ''control simulation'' for the purposes of this study.

Total (72 h) precipitation over the full domain of all of the model simulations is shown in Fig. 2, with a zoomed-in examination over Colorado provided in Fig. 3.

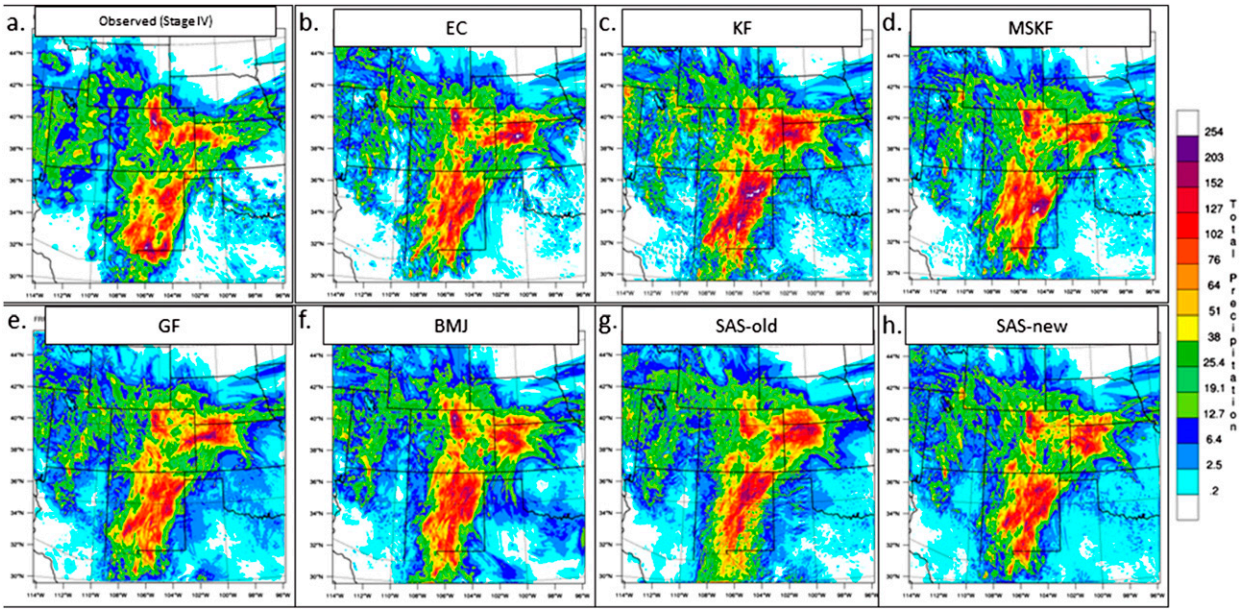

FIG. 2. The 72-h total precipitation (mm; shaded as in color bar at right) for (a) Stage-IV analysis, (b) EC, (c) KF, (d) MSKF, (e) GF, (f) BMJ, (g) SAS-old, and (h) SAS-new WRF simulations.

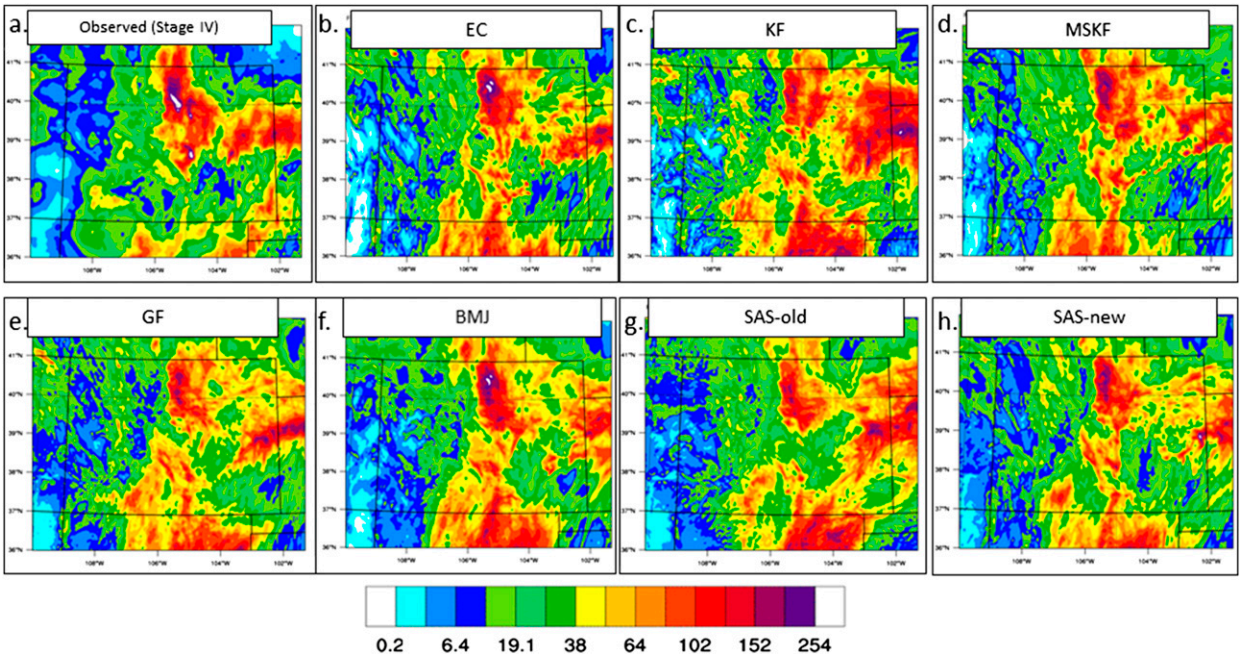

FIG. 3. As in Fig. 2, but zoomed-in to Colorado.

Simulated precipitation variability is examined with particular focus on the main regions of observed heavy precipitation: the Colorado Front Range (COFR; also referred to as downstream, and where major flooding impacts were experienced) and eastern New Mexico (ENM), also referred to as upstream relative to the generally southerly low-level flow and moisture transport throughout this event. Total precipitation differences between experimental (CP) members and the control (EC) simulation are significant over these areas in particular (Figs. 4, 5); considerable variability is also observed across runs over the Colorado–Kansas border as well. Perhaps most notably, the KF, GF, and SAS-old schemes all generate far less precipitation (>100-mm difference) in the heavily flood-impacted COFR relative to the EC simulation and observations (Figs. 5a,c,e).

With observed CAPE values not exceeding $\sim$200 J kg^{-1} in the Albuquerque, New Mexico, soundings and never exceeding 500 J kg^{-1} in the Denver, Colorado, soundings from 11 to 13 September 2013 [see Gochis et al. (their Fig. 5) and archived NM soundings from http://weather.uwyo.edu], neither the up- nor downstream environments were characterized by particularly high instability. Thus, one may expect limited convective activity and yet many of the CPSs employed produce a strong response. The KF (Fig. 6a) and SAS-old (Fig. 6e) schemes in particular (and to a lesser extent GF; Fig. 6c) generate considerable convective precipitation (i.e., precipitation produced by the CPS) over NM, while the CP-employing simulations that more closely match observations (e.g., MSKF, GF, BMJ, and SAS-new) simply do not activate as much in this region, and rather allow explicit processes to handle the bulk of precipitation generation on the grid scale (Fig. 4). This suggests that these schemes may incorporate at least some important scale-aware properties (the benefits of which are discussed previously). Though not the focus of this particular study, other studies document targeted upgrades to particular schemes that are likely driving some of the observed reduction in precipitation error: for instance, the MSKF has incorporated many scale-aware improvements as detailed above and in Zheng et al. (2016), and the SAS-new scheme incorporates convective momentum transport, which may benefit simulated upstream precipitation generation and propagation (e.g., Mahoney et al. 2009).

Examining more carefully the relative contribution of convective precipitation to total precipitation in the ENM areas of heaviest simulated upstream precipitation (cf. Figs. 4, 6, 7) suggests that for some of the CP experiments, upstream CPS activity may be linked to significant downstream model error. Based on these regional (i.e., upstream/ENM vs downstream/COFR) differences in convective versus explicit precipitation, as well as previous work linking CP scheme activity to downstream precipitation errors (Mahoney and Lackmann 2007), it is thus hypothesized that CPSs demonstrating significant CPS activity on upstream precipitation in New

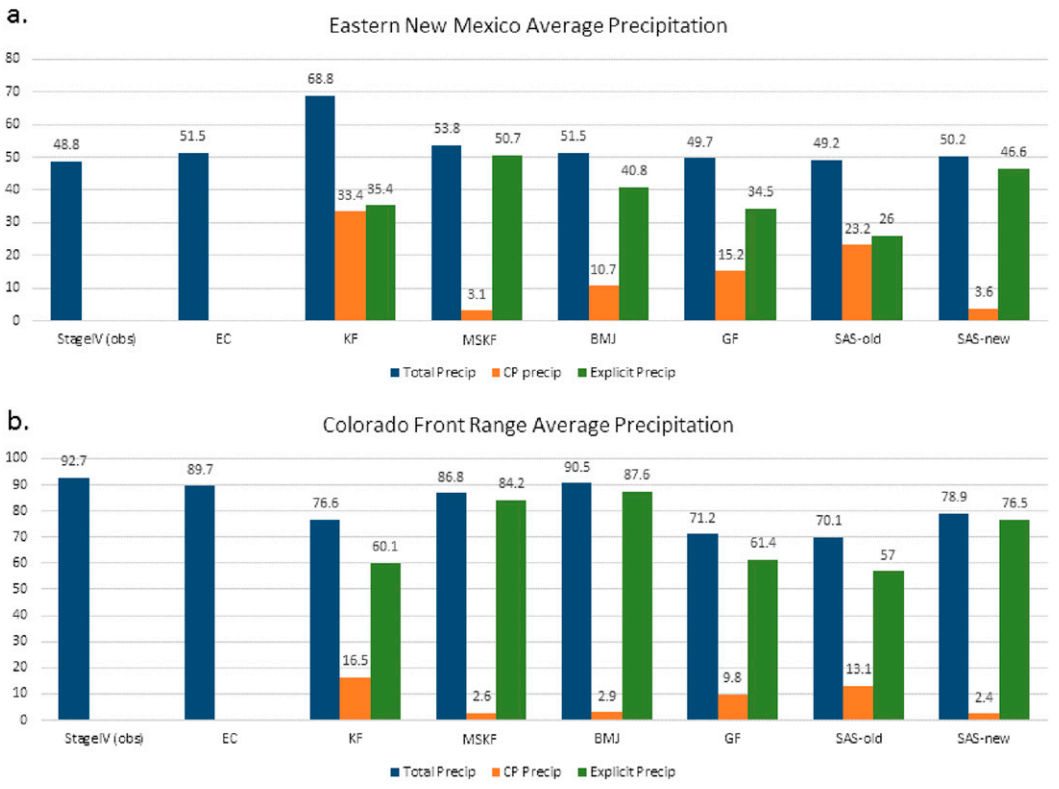

FIG. 4. Average 72-h accumulated precipitation (mm, as indicated on *y* axis) for (a) ENM (region 1 in Fig. 1) and (b) COFR (region 2 in Fig. 1.) Total precipitation is shown in blue for all model simulations; CP (explicit) precipitation is shown in orange (green) for all of the CP model experiments. Numbers above each bar denote average precipitation value in mm.

Mexico may have introduced detrimental influences on downstream precipitation over the COFR.

b. *Upstream and downstream differences between the EC, KF, and MSKF simulations*

As the precipitation differences of primary interest between the upstream and downstream regions are most clearly demonstrated in comparisons of the KF and EC simulations, a short but more in-depth analysis is devoted to those simulations here. As described in depth by Herwehe et al. (2014), Alapaty et al. (2015), and Zheng et al. (2016), the MSKF scheme was designed with the express purpose of adding scale-aware functionality, and so it is also examined alongside the KF and EC simulations. As illustrated in Figs. 6 and 7, the MSKF scheme is much less active than the KF scheme and, therefore, the MSKF simulation looks quite similar to the EC simulation in many respects. The scale-aware modifications to the MSKF scheme result in considerably less CP activity over the whole domain relative to the other CPSs (Fig. 7), and MSKF convective precipitation amounts are much reduced especially relative to the original KF scheme (Figs. 6a,b). Thus, the EC, KF, and MSKF simulations are compared in greater depth below in order to highlight some key differences between explicit convection, standard CP, and scale-aware CP for this case.

Precipitation evolution in the COFR begins to differ markedly between the KF and EC simulations around 0600 UTC 12 September 2013 (30 h into the simulation period) and continues to diverge particularly across COFR and ENM through ~1800 UTC 12 September 2013 (42 h into the simulation period) (Fig. 8). The EC and MSKF simulations both generate considerably heavy, sustained precipitation focused in the COFR region during this period (hourly rain rates $> 10\,\text{mm}\,\text{h}^{-1}$ for 12+ hours). This same intensity and distribution of precipitation is also reflected in observations (e.g., Hamill 2014; Gochis et al. 2015). However, the KF simulation focuses its heaviest precipitation across northeastern New Mexico and along the Colorado–Kansas border during this critical period (Fig. 8b), missing nearly all of the sustained, heavy rainfall in the COFR. Particularly at 1800 UTC 12 September, the heavy convective precipitation upstream across central-eastern New Mexico in the KF simulation is at odds with the EC and MSKF simulations (Figs. 8d,e,f), as well as with observations (not shown).

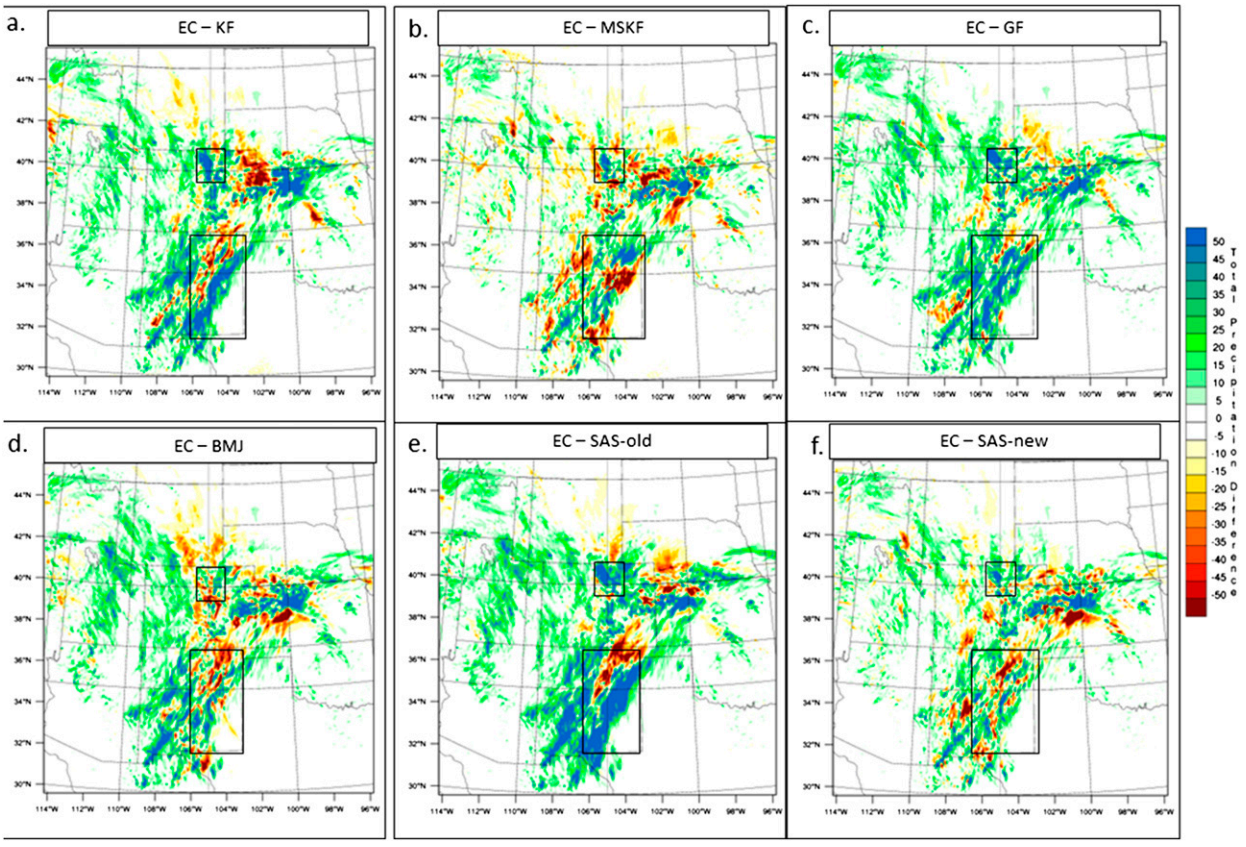

FIG. 5. The 72-h total precipitation differences (mm; shaded as indicated by color bar at right) for (a) EC − KF, (b) EC − MSKF, (c) EC − GF, (d) EC − BMJ, (e) EC − SAS-old, and (f) EC − SAS-new simulations. Red (blue) shading indicates EC precipitation < (>) CP-experiment precipitation. Black boxes indicate averaging regions used in Fig. 4 (top box is COFR; bottom box is ENM).

Low-level potential vorticity (PV) can provide insight into the ''footprint'' that heavy precipitation may have on low-level dynamic fields (e.g., Lackmann 2002; Brennan et al. 2008). Low-level (850–650 hPa) PV at 1200 UTC 12 September (which falls in the middle of the two times shown in Fig. 8) shows the influence of the simulated precipitation across the model runs (Fig. 9). The heavy convective precipitation simulated by KF in ENM and along the Colorado–Kansas border produces a consolidated, low-level PV maximum in eastern Colorado. The latent heat release and subsequent dynamical response associated with this convective precipitation also affects the surface pressure pattern, both deepening an area of surface low pressure under the PV maximum and strengthening the inverted ridge to the west of the low-level PV maximum and the precipitation itself. These differences are consistent with the diminished forcing for precipitation in the COFR (e.g., decreased upslope flow) and explain the enhanced forcing for precipitation farther to the northeast over northeast Colorado and southwestern Nebraska in the KF simulation (Figs. 8b,e). In contrast to the KF simulation, the EC and MSKF simulations lack the erroneous low-level PV maximum over eastern Colorado and are thus able to sustain the low-level easterly flow in the COFR, which provides dynamical support for prolonged upslope precipitation as observed (Fig. 9). The sequence of events described here is also very consistent with previous studies linking upstream precipitation errors to divergence in downstream mesoscale processes that ultimately affect the downstream precipitation forecast as well (e.g., Mahoney and Lackmann 2006, 2007; Baxter et al. 2011).

Moisture flux and moisture transport are also clearly affected by the differences indicated above. Low-level (700 hPa) moisture flux at 1800 UTC 12 September 2013 illustrates the eastward displacement in the KF simulation of the region of strongest moisture transport over eastern Colorado, while the EC and MSKF simulations (along with observations) focus sustained moisture flux along the COFR during this period (Fig. 10). Differences in vertically-integrated water vapor transport (IVT) also highlight how the redirected low–midlevel flow in the KF simulation over ENM leads to eastward-displaced IVT maxima both upstream in New Mexico

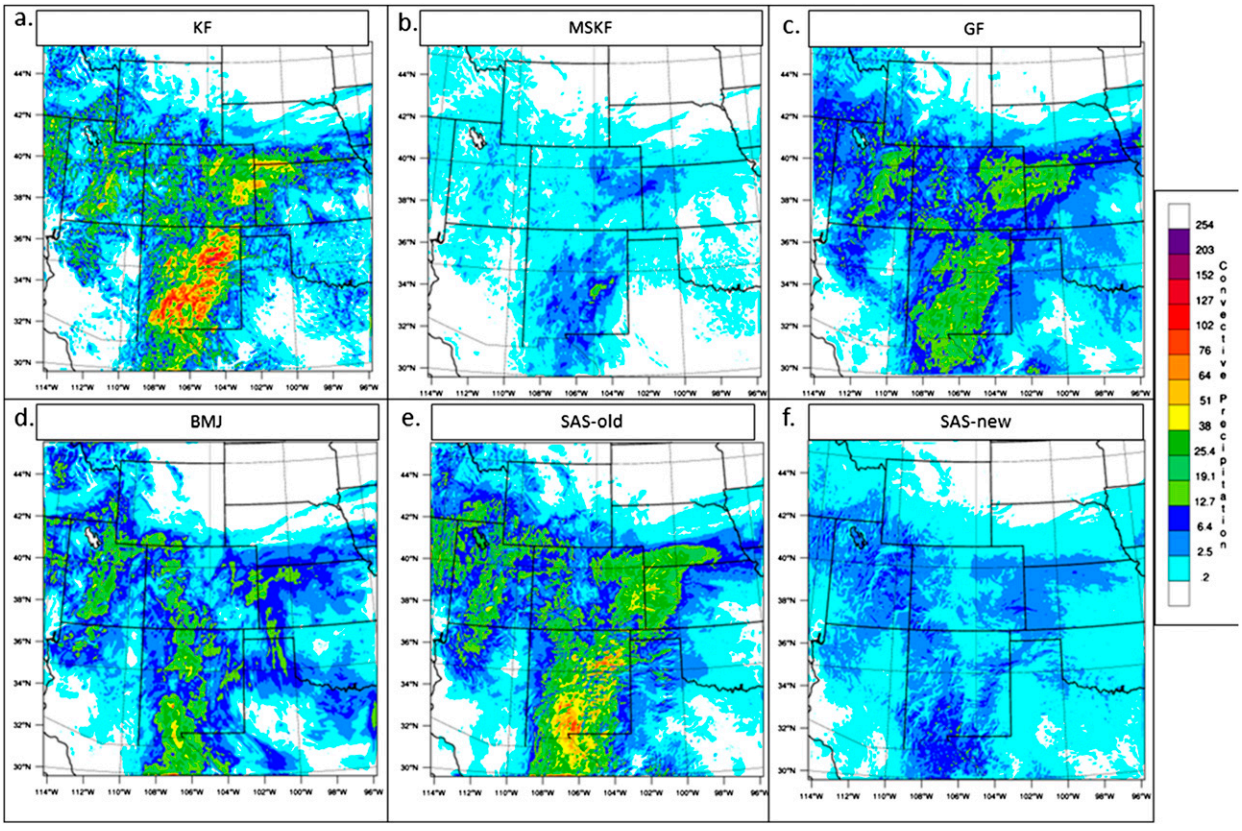

FIG. 6. The 72-h convective precipitation (mm; shaded as indicated by color bar at right) for (a) KF, (b) MSKF, (c) GF, (d) BMJ, (e) SAS-old, and (f) SAS-new simulations. (EC simulation has no convective precipitation.)

and downstream over western Kansas and northeastern Colorado (Fig. 11). The KF IVT maximum over western Kansas in particular (Fig. 11b) further demonstrates how upstream dynamical changes from convective precipitation altered the moisture transport field for all areas downstream. Finally, 60-h time integration of the vertically integrated moisture transport also highlights how such differences manifest over a longer period to overemphasize moisture transport across eastern New Mexico and northeastern Colorado in the KF simulation (Fig. 12). While differences in time-integrated IVT are subtle in the COFR due to the long-duration nature of the event, the preceding analysis (e.g., Figs. 9, 10, 11) demonstrates how the ENM upstream precipitation and evolution of the low-level dynamical environment ultimately prevented the KF simulation from being able to focus moisture sufficiently westward into the COFR upslope flow regime during the critical flood-producing precipitation period as observed.

4. Conclusions

Model simulations of the 2013 Front Range flood using 4-km horizontal grid spacing suggest that precipitation amounts in the severely flooded Colorado Front Range are dependent on model treatment of precipitation upstream. As 4-km grid spacing is considered by some to be in the convective gray zone, experiments are run using six different CPSs: KF, MSKF, GF, BMJ, SAS-old, and SAS-new. Large sensitivity is found in CPS choice with respect to the amount of precipitation generated in the Colorado Front Range (COFR) and eastern New Mexico (ENM) in particular. The KF, GF, and SAS-old schemes all generate far less precipitation (>100-mm difference) in the COFR relative to the EC simulation and observations. The KF and SAS-old schemes in particular (and to a lesser extent GF) generate considerable convective precipitation over NM. The relative contribution of CPS-generated precipitation to total precipitation in ENM in particular suggests that greater CPS activity upstream may have led to significant downstream model error. The EC, KF, and MSKF simulations are explored in greater depth to elucidate how differences in CPS-generated precipitation may have led to downstream model errors.

Analyses of low-level PV and moisture transport provide insight into how upstream precipitation differences produce lasting differences in the surrounding

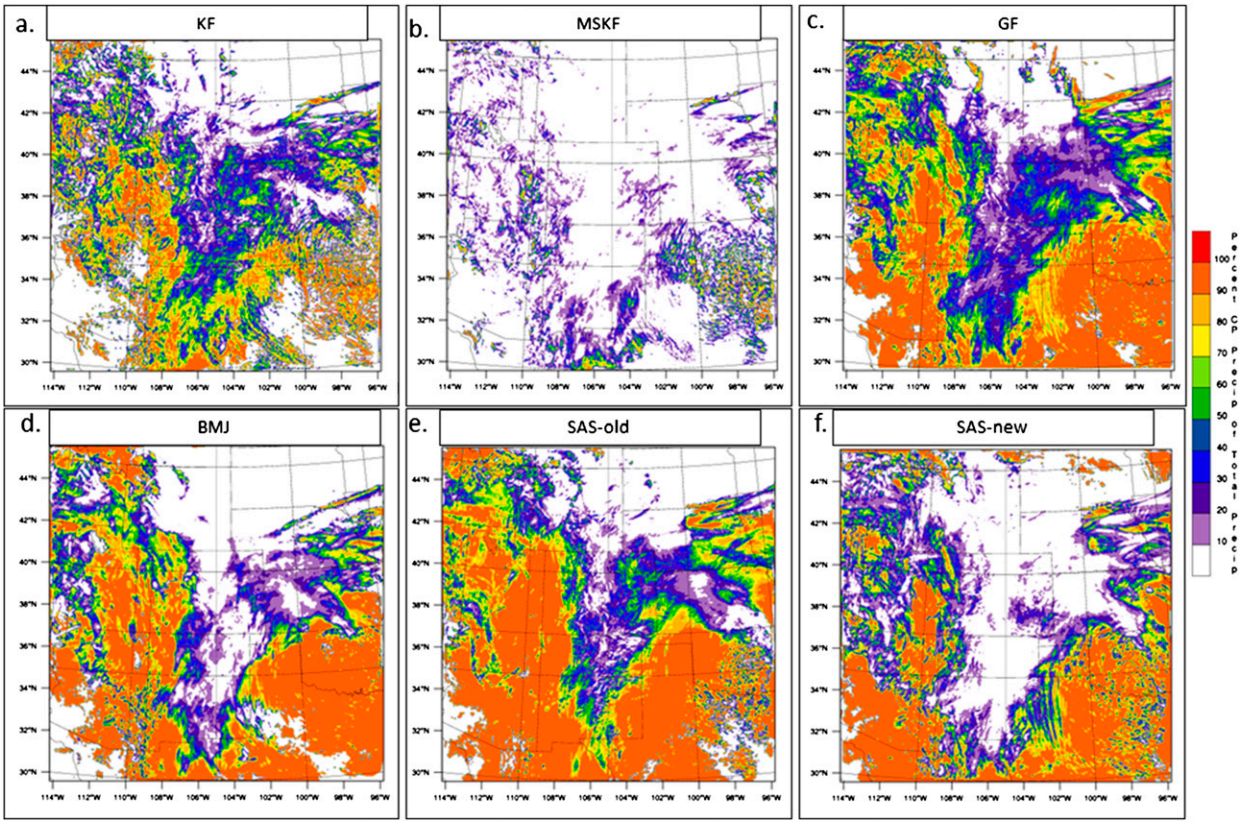

FIG. 7. Ratio of 72-h total precipitation generated by CPS relative to total precipitation (%; shaded as indicated by color bar at right) for (a) KF, (b) MSKF, (c) GF, (d) BMJ, (e) SAS-old, and (f) SAS-new simulations. (EC simulation has no convective precipitation and thus has a uniform 0% value.)

environment and affect the generation of precipitation downstream. Heavy convective precipitation simulated by KF in eastern New Mexico and Colorado produces a consolidated, low-level PV maximum in eastern Colorado. This leads to a strengthening of the inverted ridge to the west, thereby decreasing precipitation in the COFR relative to the EC and MSKF simulations, as well as observations. The alteration of low-level flow by the KF-produced low-level PV maximum also deepens the trough/low to the east over northeast Colorado/western Kansas and increases precipitation there. Moisture flux maxima are also accordingly eastwardly displaced in the KF simulation, while the EC and MSKF simulations (along with observations) focus sustained moisture flux into the steep terrain of the COFR, the result of which was some of the most intense rainfall and flooding observed during the event. At least for this single case study, it appears that the updates implemented by the MSKF have successfully adapted the KF scheme to be more scale aware and less prone to overactivity; similar results are found for other space and time scales in Alapaty et al. (2015) and Zheng et al. (2016).

Precipitation differences on the scales observed here underscore the need to carefully consider the suitability of CP for a given modeling system design, even at 4-km grid spacing. For the 2013 Front Range floods in particular, Hamill (2014) hypothesizes that the choice of model physics may have been the ultimate source for the glaring precipitation forecast differences found both among the NOAA Short-Range Ensemble Forecast (SREF) system membership as well as in comparison with other model forecasts systems of similar resolution. That 1) the experiments conducted here were run as simulations (i.e., boundaries were updated with analyzed—and not forecast—conditions), and 2) a horizontal grid spacing of 4 km would be expected to generate most precipitation explicitly, it seems particularly significant, and perhaps surprising, that the choice of CPS at these space and time scales would still cause 3-day precipitation differences to exceed 100 mm in several of the most heavily flood-impacted regions.

Model performance in the convective physics gray zone is likely very case dependent. This singular analysis of a high-impact flooding case suggests that model skill may be acutely lost when employing a CPS

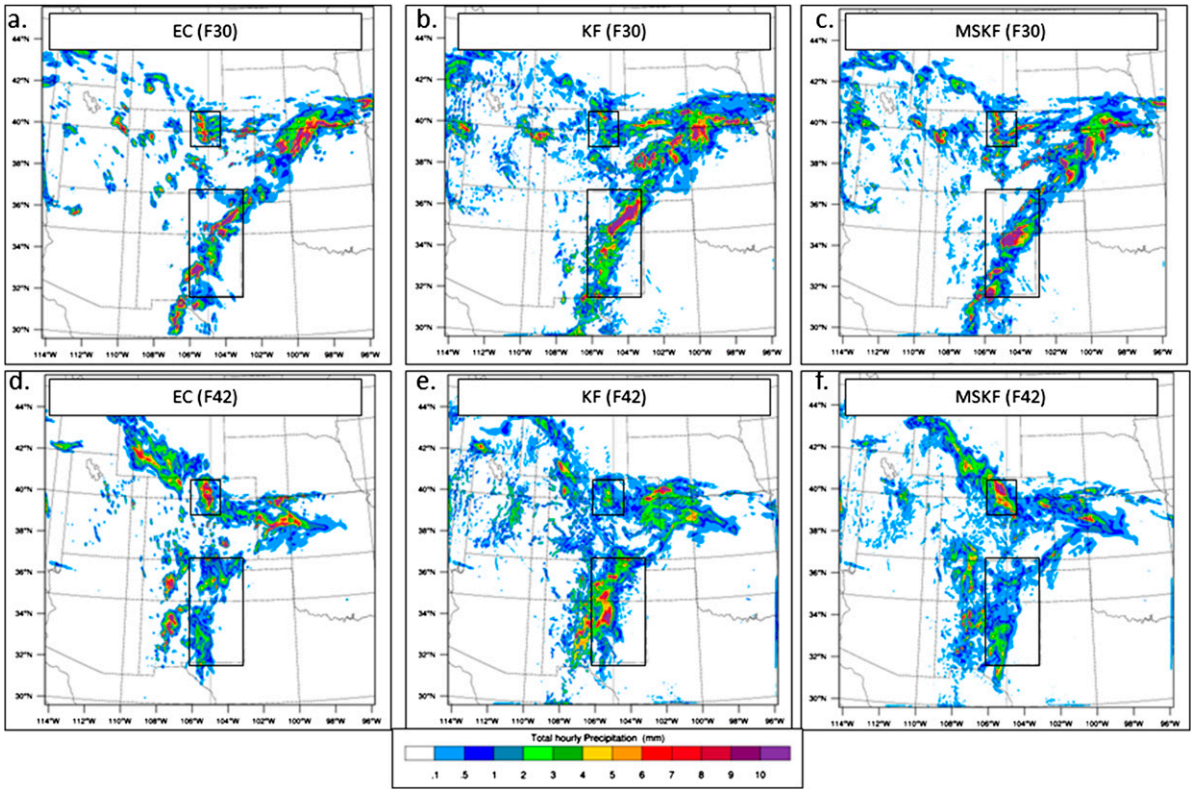

FIG. 8. (a) EC-simulated hourly precipitation (mm; shaded as indicated by color bar at bottom) ending 0600 UTC 12 Sep (30 h into simulation, denoted "F30"); (b) as in (a), but for KF; (c) as in (a), but for MSKF; (d) as in (a), but ending at 1800 UTC 12 Sep (42 h into simulation, denoted "F42"); (e) as in (d), but for KF; (f) as in (d), but for MSKF. Black boxes illustrate regions highlighted in text (top box is upstream/COFR; bottom box is downstream/ENM).

that has not been adapted to be "scale-aware." Given that most operational and proposed convection-allowing ensembles operate at precisely this ~4-km scale, it is critical to understand the types of cases and environments in which assumptions applied by a given CPS may fail.

It is conceivable, and many studies have shown, that CPSs in the model physics gray zone can help increase

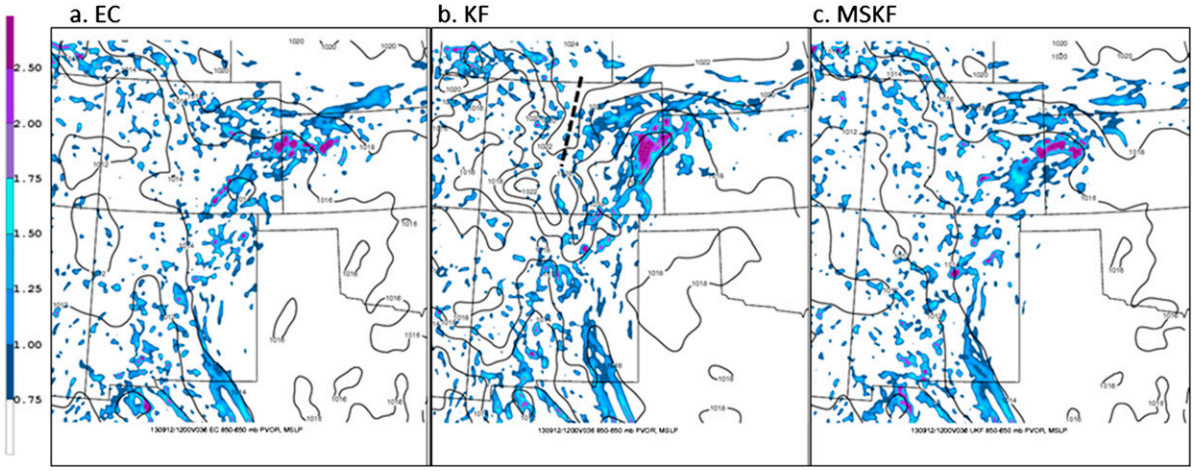

FIG. 9. (a) EC-simulated 850–650-hPa layer-averaged PV [PVU (1 PVU = 10^{-6} K kg^{-1} m^2 s^{-1}); shaded as in color bar at left] and (terrain-corrected) sea level pressure (hPa; black contours as labeled) valid at 1200 UTC 12 Sep (36 h into simulation period); (b) as in (a), but for KF; and (c) as in (a), but for MSKF. Black dashed line in (b) denotes the location of the inverted ridge.

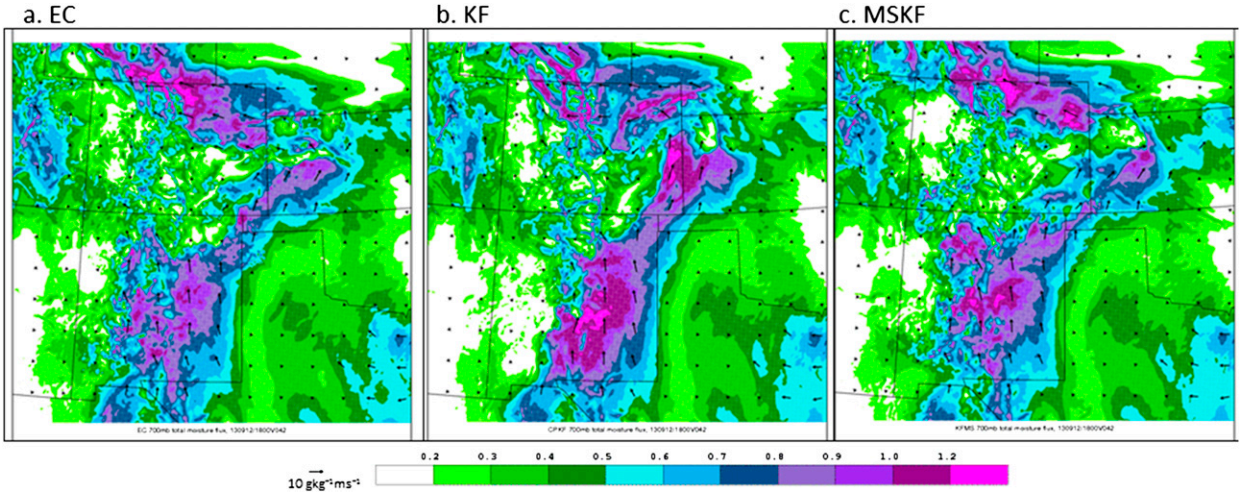

FIG. 10. (a) EC-simulated 700-hPa moisture flux ($\times 10\,\mathrm{g\,kg^{-1}\,m\,s^{-1}}$; shaded as in color bar at bottom and vectors with reference vector as indicated to left of color bar) valid at 1800 UTC 12 Sep (42 h into simulation period); (b) as in (a), but for KF; and (c) as in (a), but for MSKF.

forecast skill particularly when integrated over long periods of time and large regions (e.g., Alapaty et al. 2015; Zheng et al. 2016). Indeed, many higher-resolution climate modeling efforts are now targeting resolutions that approach or meet convection-allowing requirements, and questions are outstanding as to whether certain aspects of a CPS will still be needed for these generally larger-domain, longer-duration simulations. However, as extreme events are generally nonlinear in nature, they will often be a fail point for model parameterizations, independent of whether the model is run as a "weather" or "climate" model. If a main objective of running convection-allowing ensembles (as opposed to convection-parameterized ensembles) is to best resolve the atmospheric processes that lead to extreme events, it may be that CP should be minimized. If a specific ensemble system construct necessitates that CP should be employed for the improvement of certain other fields, perhaps a portion of model members could be run explicitly so as to allow the user (e.g., forecaster or researcher) to differentiate sets of model solutions based on convective treatment—and thus use their experience and intuition as to which may be more skillful in a given situation (particularly those of potentially extreme precipitation.)

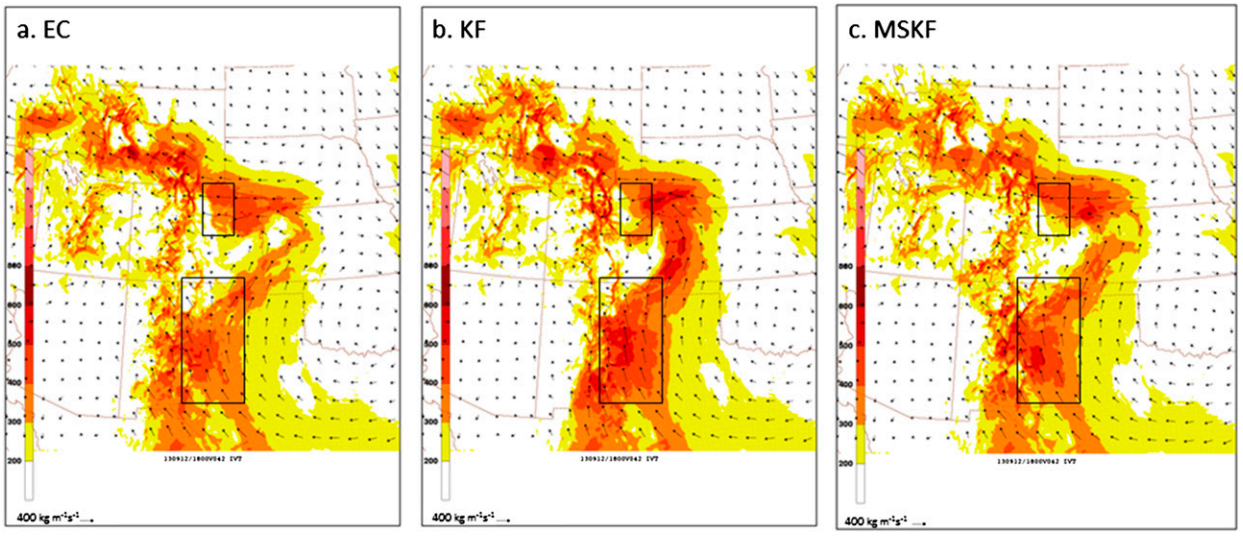

FIG. 11. (a) EC-simulated surface − 200 hPa IVT ($\mathrm{kg\,m^{-1}\,s^{-1}}$; shaded as in color bar and in vectors, where reference vector in lower left represents $400\,\mathrm{kg\,m^{-1}\,s^{-1}}$) valid at 1800 UTC 12 Sep (42 h into simulation period); (b) as in (a), but for KF; and (c) as in (a), but for MSKF. Black boxes illustrate regions highlighted in text (top box is upstream/COFR; bottom box is downstream/ENM).

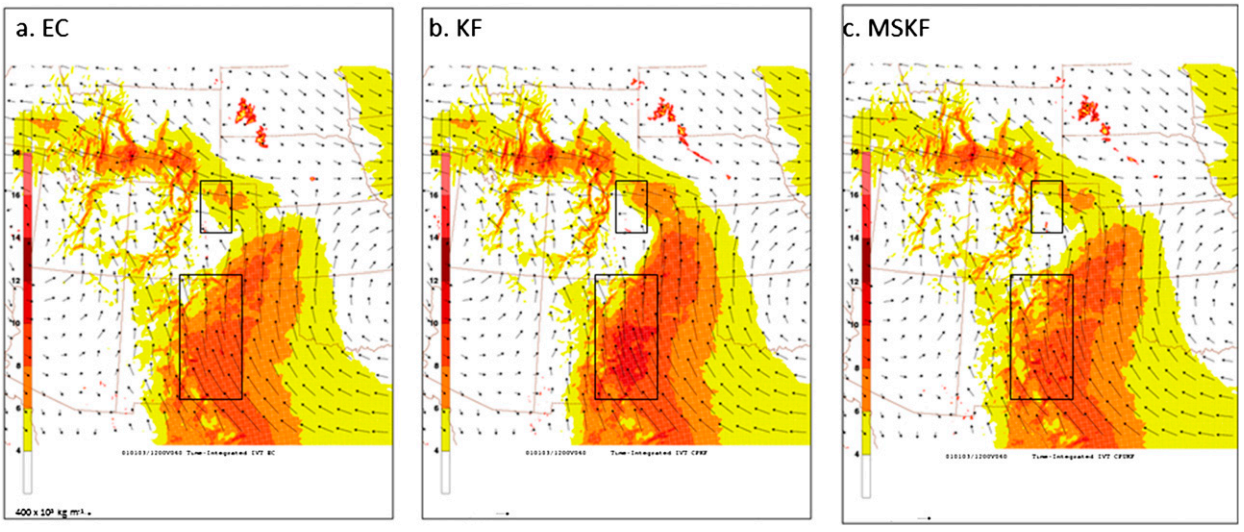

FIG. 12. Surface − 200 hPa IVT, time integrated from 0000 UTC 11 Sep to 1200 UTC 13 Sep 2013 (10^6 kg m^{-1}; shaded as in color bar and in vectors, where reference vector in lower left represents 400×10^5 kg m^{-1}); (b) as in (a), but for KF; and (c) as in (a), but for MSKF. Black boxes illustrate regions highlighted in text (top box is upstream/COFR; bottom box is downstream/ENM).

While this is but a single case study of one extreme event, the differences caused by the gray-zone decision to employ or not employ CP led to significant differences in simulated precipitation in an area that was in the end ravaged by high-impact flooding. The degree of impact suggests that, despite decades of research into this general topic of CP in the gray zone, increased demand for both scale-aware convective physics and convection-allowing ensembles will likely require renewed consideration of CP treatment in an evolving—but still present—model physics gray zone.

Acknowledgments. This publication was supported by the Physical Sciences Division, NOAA/ESRL. Professor Gary Lackmann of North Carolina State University; Dr. Rob Cifelli of the Physical Sciences Division, NOAA/ESRL; and three anonymous reviewers are acknowledged for providing valuable comments on the manuscript. NCAR and the National Science Foundation (NSF) are acknowledged for the availability of the WRF Model, NCL software, and GEMPAK software. Software support was also provided by Ben Moore (SUNY-Albany) and Prof. Shawn Milrad (Embry-Riddle).

REFERENCES

Alapaty, K., J. A. Herwehe, O. R. Bullock Jr., Y. Zheng, A. Sims, M. S. Mallard, and L. Fowler, 2015: Testing of Multi-Scale Kain–Fritsch scheme using Regional and Global Models. *16th Annual WRF Users' Workshop*, Boulder, CO, EPA, 7.4. [Available online at http://www2.mmm.ucar.edu/wrf/users/workshops/WS2015/ppts/7.4.pdf.]

Baxter, M. A., P. N. Schumacher, and J. M. Boustead, 2011: The use of potential vorticity inversion to evaluate the effect of precipitation on downstream mesoscale processes. *Quart. J. Roy. Meteor. Soc.*, **137**, 179–198, doi:10.1002/qj.730.

Bengtsson, L., and H. Körnich, 2016: Impact of a stochastic parametrization of cumulus convection, using cellular automata, in a mesoscale ensemble prediction system. *Quart. J. Roy. Meteor. Soc.*, **142**, 1150–1159, doi:10.1002/qj.2720.

——, S. Tijm, F. Váňa, and G. Svensson, 2012: Impact of flow-dependent horizontal diffusion on resolved convection in AROME. *J. Appl. Meteor. Climatol.*, **51**, 54–67, doi:10.1175/JAMC-D-11-032.1.

Brennan, M. J., G. M. Lackmann, and K. M. Mahoney, 2008: Potential vorticity (PV) thinking in operations: The utility of nonconservation. *Wea. Forecasting*, **23**, 168–182, doi:10.1175/2007WAF2006044.1.

Bryan, G. H., J. C. Wyngaard, and J. M. Fritsch, 2003: Resolution requirements for the simulation of deep moist convection. *Mon. Wea. Rev.*, **131**, 2394–2416, doi:10.1175/1520-0493(2003)131<2394:RRFTSO>2.0.CO;2.

Bukovsky, M. S., J. S. Kain, and M. E. Baldwin, 2006: Bowing convective systems in a popular operational model: Are they for real? *Wea. Forecasting*, **21**, 307–324, doi:10.1175/WAF908.1.

Cintineo, R., J. A. Otkin, M. Xue, and F. Kong, 2014: Evaluating the performance of planetary boundary layer and cloud microphysical parameterization schemes in convection-permitting ensemble forecasts using synthetic *GOES-13* satellite observations. *Mon. Wea. Rev.*, **142**, 163–182, doi:10.1175/MWR-D-13-00143.1.

Clark, A. J., W. A. Gallus, M. Xue, and F. Kong, 2009: A comparison of precipitation forecast skill between small convection-allowing and large convection-parameterizing ensembles. *Wea. Forecasting*, **24**, 1121–1140, doi:10.1175/2009WAF2222222.1.

——, and Coauthors, 2012: An overview of the 2010 Hazardous Weather Testbed Experimental Forecast Program Spring Experiment. *Bull. Amer. Meteor. Soc.*, **93**, 55–74, doi:10.1175/BAMS-D-11-00040.1.

Deng, A., and D. R. Stauffer, 2006: On improving 4-km mesoscale model simulations. *J. Appl. Meteor. Climatol.*, **45**, 361–381, doi:10.1175/JAM2341.1.

Done, J., C. Davis, and M. Weisman, 2004: The next generation of NWP: Explicit forecasts of convection using the Weather Research and Forecasting (WRF) model. *Atmos. Sci. Lett.*, **5**, 110–117, doi:10.1002/asl.72.

Friedrich, K., E. A. Kalina, J. Aikins, M. Steiner, D. Gochis, P. A. Kucera, K. Ikeda, and J. Sun, 2016: Raindrop size distribution and rain characteristics during the 2013 Great Colorado Flood. *J. Hydrometeor.*, **17**, 53–72, doi:10.1175/JHM-D-14-0184.1.

Gerard, L., 2015: Bulk mass-flux perturbation formulation for a unified approach of deep convection at high resolution. *Mon. Wea. Rev.*, **143**, 4038–4063, doi:10.1175/MWR-D-15-0030.1.

Gochis, D., and Coauthors, 2015: The Great Colorado Flood of September 2013. *Bull. Amer. Meteor. Soc.*, **96**, 1461–1487, doi:10.1175/BAMS-D-13-00241.1.

Golding, B., N. Roberts, G. Leoncini, K. Mylne, and R. Swinbank, 2016: MOGREPS-UK convection-permitting ensemble products for surface water flood forecasting: Rationale and first results. *J. Hydrometeor.*, **17**, 1383–1406, doi:10.1175/JHM-D-15-0083.1.

Grell, G. A., and S. Freitas, 2013: A scale and aerosol aware stochastic convective parameterization for weather and air quality modeling. *Atmos. Chem. Phys. Discuss.*, **13**, 23 845–23 893, doi:10.5194/acpd-13-23845-2013.

Hamill, T. M., 2014: Performance of operational model precipitation forecast guidance during the 2013 Colorado Front-Range floods. *Mon. Wea. Rev.*, **142**, 2609–2618, doi:10.1175/MWR-D-14-00007.1.

Han, J., and H.-L. Pan, 2011: Revision of convection and vertical diffusion schemes in the NCEP Global Forecast System. *Wea. Forecasting*, **26**, 520–533, doi:10.1175/WAF-D-10-05038.1.

Herwehe, J. A., K. Alapaty, and O. R. Bullock Jr., 2014: Evaluation of developments toward a multi-scale Kain-Fritsch parameterization in WRF. *2014 Community Modeling and Analysis System Conf.*, Chapel Hill, NC, EPA. [Available online at https://www.cmascenter.org/conference//2014/slides/jerry_herwehe_evaluation_developments_2014.pdf.]

Janjić, Z. I., 1994: The step-mountain eta coordinate model: Further developments of the convection, viscous sublayer, and turbulence closure schemes. *Mon. Wea. Rev.*, **122**, 927–945, doi:10.1175/1520-0493(1994)122<0927:TSMECM>2.0.CO;2.

Kain, J. S., and J. M. Fritsch, 1993: Convective parameterization for mesoscale models: The Kain–Fritsch scheme. *The Representation of Cumulus Convection in Numerical Models, Meteor. Monogr.*, No. 24, Amer. Meteor. Soc., 165–170.

——, and Coauthors, 2008: Some practical considerations regarding horizontal resolution in the first generation of operational convection-allowing NWP. *Wea. Forecasting*, **23**, 931–952, doi:10.1175/WAF2007106.1.

Kuo, Y. H., J. Bresch, M.-D. Cheng, J. Kain, D. B. Parsons, W.-K. Tao, and D.-L. Zhang, 1997: Summary of a mini-workshop on cumulus parameterization for mesoscale models. *Bull. Amer. Meteor. Soc.*, **78**, 475–491.

Lackmann, G. M., 2002: Cold-frontal potential vorticity maxima, the low-level jet, and moisture transport in extratropical cyclones. *Mon. Wea. Rev.*, **130**, 59–74, doi:10.1175/1520-0493(2002)130<0059:CFPVMT>2.0.CO;2.

——, 2011: *Midlatitude Synoptic Meteorology: Dynamics, Analysis, and Forecasting*. Amer. Meteor. Soc., 345 pp.

Lavers, D. A., and G. Villarini, 2013: Were global numerical weather prediction systems capable of forecasting the extreme Colorado rainfall of 9–16 September 2013? *Geophys. Res. Lett.*, **40**, 6405–6410, doi:10.1002/2013GL058282.

Lean, H. W., P. A. Clark, M. Dixon, N. M. Roberts, A. Fitch, R. Forbes, and C. Halliwell, 2008: Characteristics of high-resolution versions of the Met Office Unified Model for forecasting convection over the United Kingdom. *Mon. Wea. Rev.*, **136**, 3408–3424, doi:10.1175/2008MWR2332.1.

Lin, Y., and K. E. Mitchell, 2005: The NCEP Stage II/IV hourly precipitation analyses: Development and applications. *19th Conf. on Hydrology*, San Diego, CA, Amer. Meteor. Soc., 1.2. [Available online at https://ams.confex.com/ams/Annual2005/techprogram/paper_83847.htm.]

Mahoney, K. M., and G. M. Lackmann, 2006: The sensitivity of numerical forecasts to convective parameterization: A case study of the 17 February 2004 East Coast cyclone. *Wea. Forecasting*, **21**, 465–488, doi:10.1175/WAF937.1.

——, and ——, 2007: The effect of upstream convection on downstream precipitation. *Wea. Forecasting*, **22**, 255–277, doi:10.1175/WAF986.1.

——, ——, and M. D. Parker, 2009: The role of momentum transport in the motion of a quasi-idealized mesoscale convective system. *Mon. Wea. Rev.*, **137**, 3316–3338, doi:10.1175/2009MWR2895.1.

——, M. Alexander, J. D. Scott, and J. Barsugli, 2013: High-resolution downscaled simulations of warm-season extreme precipitation events in the Colorado Front Range under past and future climates. *J. Climate*, **26**, 8671–8689, doi:10.1175/JCLI-D-12-00744.1.

——, F. M. Ralph, K. Wolter, N. Doesken, M. Dettinger, D. Gottas, and A. White, 2015: Climatology of extreme daily precipitation in Colorado and its diverse spatial and seasonal variability. *J. Hydrometeor.*, **16**, 781–792, doi:10.1175/JHM-D-14-0112.1.

——, J. J. Lukas, and B. McCormick, 2016: Examining terrain elevation assumptions used in current extreme precipitation estimation practices: A modeling study of the 2013 Colorado Front Range floods. *30th Conf. on Hydrology*, New Orleans, LA, Amer. Meteor. Soc., J13.2. [Available online at https://ams.confex.com/ams/96Annual/webprogram/Paper289370.html.]

Molinari, J., and M. Dudek, 1992: Parameterization of convective precipitation in mesoscale numerical models: A critical review. *Mon. Wea. Rev.*, **120**, 326–344, doi:10.1175/1520-0493(1992)120<0326:POCPIM>2.0.CO;2.

Morales, A., R. S. Schumacher, and S. M. Kreidenweis, 2015: Mesoscale vortex development during extreme precipitation: Colorado, September 2013. *Mon. Wea. Rev.*, **143**, 4943–4962, doi:10.1175/MWR-D-15-0086.1.

Pan, H.-L., and W.-S. Wu, 1995: Implementing a mass flux convective parameterization package for the NMC medium-range forecast model. NMC Office Note 409, 40 pp. [Available from NCEP/EMC, 5200 Auth Road, Camp Springs MD 20746.]

Petch, J. C., A. R. Brown, and M. E. B. Gray, 2002: The impact of horizontal resolution on the simulations of convective development over land. *Quart. J. Roy. Meteor. Soc.*, **128**, 2031–2044, doi:10.1256/003590002320603511.

Saha, S., and Coauthors, 2010: The NCEP Climate Forecast System Reanalysis. *Bull. Amer. Meteor. Soc.*, **91**, 1015–1057, doi:10.1175/2010BAMS3001.1.

Schwartz, C. S., 2014: Reproducing the September 2013 record-breaking rainfall over the Colorado Front Range with

high-resolution WRF forecasts. *Wea. Forecasting*, **29**, 393–402, doi:10.1175/WAF-D-13-00136.1.

——, G. S. Romine, R. A. Sobash, K. R. Fossell, and M. L. Weisman, 2015: NCAR's experimental real-time convection-allowing ensemble prediction system. *Wea. Forecasting*, **30**, 1645–1654, doi:10.1175/WAF-D-15-0103.1.

Seaman, N. L., S. A. Michelson, P. C. Shafran, and D. R. Stauffer, 1998: Forecast of a severe squall line development in MM5 using explicit moist physics at 4-km resolution. Preprints, *12th Conf. on Numerical Weather Prediction*, Phoenix, AZ, Amer. Meteor. Soc., J1–J4.

Skamarock, W. C., and Coauthors, 2008: A description of the Advanced Research WRF version 3. NCAR Tech. Note NCAR/TN-475+STR, 113 pp., doi:10.5065/D68S4MVH.

Weisman, M. L., W. C. Skamarock, and J. B. Klemp, 1997: The resolution dependence of explicitly modeled convective systems. *Mon. Wea. Rev.*, **125**, 527–548, doi:10.1175/1520-0493(1997)125<0527:TRDOEM>2.0.CO;2.

——, C. Davis, W. Wang, K. W. Manning, and J. B. Klemp, 2008: Experiences with 0–36-h explicit convective forecasts with the WRF-ARW model. *Wea. Forecasting*, **23**, 407–437, doi:10.1175/2007WAF2007005.1.

Zhang, D.-L., E.-Y. Hsie, and M. W. Moncrieff, 1988: A comparison of explicit and implicit predictions of convective and stratiform precipitating weather systems with a meso-β-scale numerical model. *Quart. J. Roy. Meteor. Soc.*, **114**, 31–60, doi:10.1002/qj.49711447903.

Zheng, Y., K. Alapaty, J. A. Herwehe, A. D. Del Genio, and D. Niyogi, 2016: Improving high-resolution weather forecasts using the Weather Research and Forecasting (WRF) Model with an updated Kain–Fritsch scheme. *Mon. Wea. Rev.*, **144**, 833–860, doi:10.1175/MWR-D-15-0005.1.